EJGE

Effect of Geogrid Reinforcement Location in Paved Road Improvement

Hossein Moayedi

Department of Civil Engineering, University Putra Malaysia, Serdang, Selangor, Malaysia
e-mail: Hossein.Moayedi@gmail.com

Sina Kazemian

Research Scholar, Department of Civil Engineering, University Putra Malaysia, Serdang, Selangor, Malaysia
e-mail: skazemian_2002@yahoo.com

Arun Prasad

Post-Doctoral, Department of Civil Engineering, University Putra Malaysia, Serdang, Selangor, Malaysia
e-mail: arun@eng.upm.edu.my

Bujang B. K. Huat

Professor, Department of Civil Engineering, University Putra Malaysia, Serdang, Selangor, Malaysia
e-mail: bujang@eng.upm.edu.my

ABSTRACT

A series of two-dimensional finite element simulations are carried out to evaluate the benefits of integrating a high modulus geogrid in a paved road. This paper describes the behavior of reinforced asphalt concrete (AC) pavement under plane strain conditions and subjected to monotonic loading. The results of improvement of paved track using geogrids are presented. Geogrid reinforcement into paved road in most cases will improve the performance of the transportation support. Analytical results for three different most possibilities of geogrid reinforcement in the paved road layers have been evaluated. The optimum position was decided based upon the tension stress absorption value, deformation reduce rate and tension cut-off point location. Three types of reinforcing model and one type of unreinforced model of paved road were selected. The results showed that tension stress absorption increases with shifting the geogrid towards the top of the pavement and attains the highest values when the geogrid is placed between asphalt layer and base layer in model.

KEYWORDS: Paved road, Geogrid, Optimal location, Tension stress absorption.

INTRODUCTION

Geosynthetic materials have been successfully used to stabilize subgrade soils in road construction, which leads to improved performance of paved and unpaved roads. The research conducted so far indicates that the geogrids perform better as a reinforcing element. Reinforced soils are often treated as a

composite material, in which the reinforcement resists tensile stresses and interacts with soil through friction. Geogrids can improve the performance of the subgrade soil through four mechanisms: prevention of local shearing of the subgrade, improvement of load distribution through the base course, reduction or reorientation of shear stresses on the subgrade, and tensioned membrane effect. Placed between the subgrade and base course, or within the base course, the geosynthetic improves the performance of paved roads. Reinforcement increases the bearing capacity of the subgrade, stiffens the base layer thereby reducing normal stresses and changing the magnitude and orientation of shear stresses on the subgrade in the loaded area, restricts lateral movement of the base course material and the subgrade soil, and can provide tensioned membrane support where deep rutting occurs (Giroud et al., 1985).

One of the beneficial effects of geosynthetic reinforcement at the interface between base course and subgrade soil is to carry the shear stresses induced by vehicular loads at the interface (Milligan and Love, 1984; Perkins, 1999). The interlocking between the geogrid and the base course aggregate results in reduced lateral movement of the base course aggregate as a result, no outward shear stresses are transmitted to the subgrade. At the same time, the bottom surface of the base course, with confined aggregate striking through geogrid apertures, provides a rough surface that resists lateral movement by the subgrade and increase the subgrade bearing capacity.

The geogrids have an elastic-plastic behavior so that they quickly react to applied loads with an increase in the elastic modulus; in the case of short term impact loading, creep phenomenon does not occur, therefore the whole tensile resistance of the geogrid can be mobilized. Further, geogrids allow an increase of the dynamic dumping characteristics of the reinforced soil compared to unreinforced soil, both through the energy that is directly absorbed by the geogrid itself and due to friction generated in the dynamic stage (Carotti and Rimoldi, 1998).

Although there is a lot of information and experience with geosynthetic reinforcement of subgrade soils, many pavement failures still occur. These failures may be due to the lack of understanding of how these materials influence the engineering properties of subgrade soils and what is the optimum position of reinforcement within a layer to derive maximum benefit.

Tension stress absorption of geogrid has changed surprisingly with change in position of the reinforcement. Some researchers believe that geogrid should be placed near the load (Chan et al., 1989), while others have found that it should be near the bottom or at mid-height (Broms, 1977). Giroud et al. (1985) showed that the geogrids could improve the performance of subgrade soil through three mechanisms, namely: confinement, improved load distribution through the base layer, and tensioned membrane effect, which reduces stresses. For pavements constructed on soft subgrades, the reinforcement should be placed at or near the bottom of the base.

Barksdale *et al.* (1989) utilized the results of a 2D finite element method to estimate the reduction in base thickness for a stiff geosynthetic. Miura et al. (1990) carried out an isotropic linear elastic FE analysis using 2D continuum elements to represent the HMA, base, subbase and subgrade layers. Dondi (1994) performed a 3D FE analysis of a pavement structure using non-linear constitutive models for the base and subgrade and a linear elastic model for the HMA and geogrid layers. Wathugala *et al.* (1996) used the ABAQUS finite element program to explore the decrease in the rut depth as a result of placing the geosynthetic membrane at the base–subgrade interface of a flexible pavement system. A series of finite element simulations are carried out to evaluate the benefits of integrating a high modulus geosynthetic into the pavement foundation. Three locations of the geosynthetic reinforcement are studied, namely the base–asphalt concrete interface, the base–subgrade interface, and inside the base layer at a

height of 1/3 of its thickness from the bottom. It is found that placing the geosynthetic reinforcement at the base–asphalt concrete interface leads to the highest reduction of the fatigue strain (46–48%).

All these findings indicate that the position of geogrid in a layer is still a subject for research. The present study was undertaken to investigate the optimum position of the geogrid in a layer of sand subgrade soil. The geogrid was placed at different positions and effectiveness of reinforcement layer was investigated through analytical modeling (Plaxis).

FINITE ELEMENT ANALYSIS

An axisymmetric analysis was carried out using Mohr-Coulomb's criterion. The parameters required for all the materials are for the calculations are presented in Table 1. The typical finite element mesh consisted of 1765 nodes and 752 15-node triangular elements. Geogrid has been used as a strain absorption interlayer system. Perkins (2001) demonstrated that in most of these analyses the geosynthetic reinforcement membrane is considered as an isotropic elastic material. Interface elements have been used at the interface of the geogrid. This will allow the relative deformation between the geogrid and gravel and sand layers. Conventional kinematic boundary conditions are adopted, i.e., roller support on all four vertical boundaries of the mesh and fixed support at the bottom of the mesh. Such boundary conditions have been successfully used by Kuo *et al.* (1995). Iterative procedure is adopted for the solution to reduce the normal out of balance force. This strain absorption interlayer system is a soft layer that is usually placed at the bottom of an HMA overlay to absorb a large portion of the energy.

The unreinforced structure was modeled for a loading of 557 kPa having a radius of 200 mm (Yoder and Witczak, 1975; Hansen *et al.*, 1989). The analysis was carried out for drained condition without pore water pressure changes. To simulate the stress dependency of the moduli, the structural layers were divided into sub-layers with the same strength parameters, but different moduli. The axisymmetric analysis was used to get a three dimensional stress distribution. The use of plain strain analysis, where the loading would have been continuous line loading, would have given an overestimation of the stresses and responses.

Table 1: Input parameters.

Material	Asphalt	Crushed Rock	Crushed Gravel	Sand
Thickness (mm)	50	200	250	1500
Elastic modulus (MPa)	5400	300-220-200	140-90	75
Poisson's ratio	0.3	0.35	0.35	0.35
Unit weight (kN/m^3)	25	21.2	22	18
Cohesion (kPa)	-	30	20	8
Friction angle (°)	-	43	44	36
Dilatation angle (°)	-	13	14	6
K_0	1	0.32	0.3	0.42

To model the surface load of the dual wheel, the total load was transferred to a circular loading with an average contact pressure (Korkiala *et al.*, 2003) as shown in Figure 1.

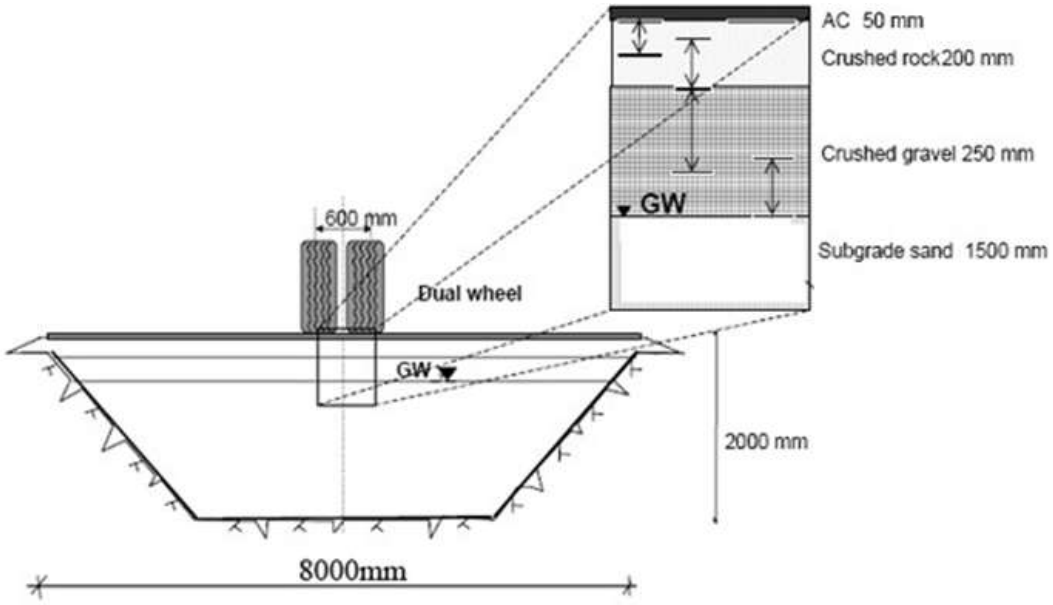

Figure 1: Element surface load of the dual wheel.

The deformation modulus of unbound material is usually strongly dependent on the stress state. The base and subbase layer were divided into thinner layers with the same strength parameters but with different modulus values. The modeling was carried out with the parameters adopted from the standard (ASTM D11241–94). The element mesh and boundary conditions of the unreinforced structure are shown in Figure 2.

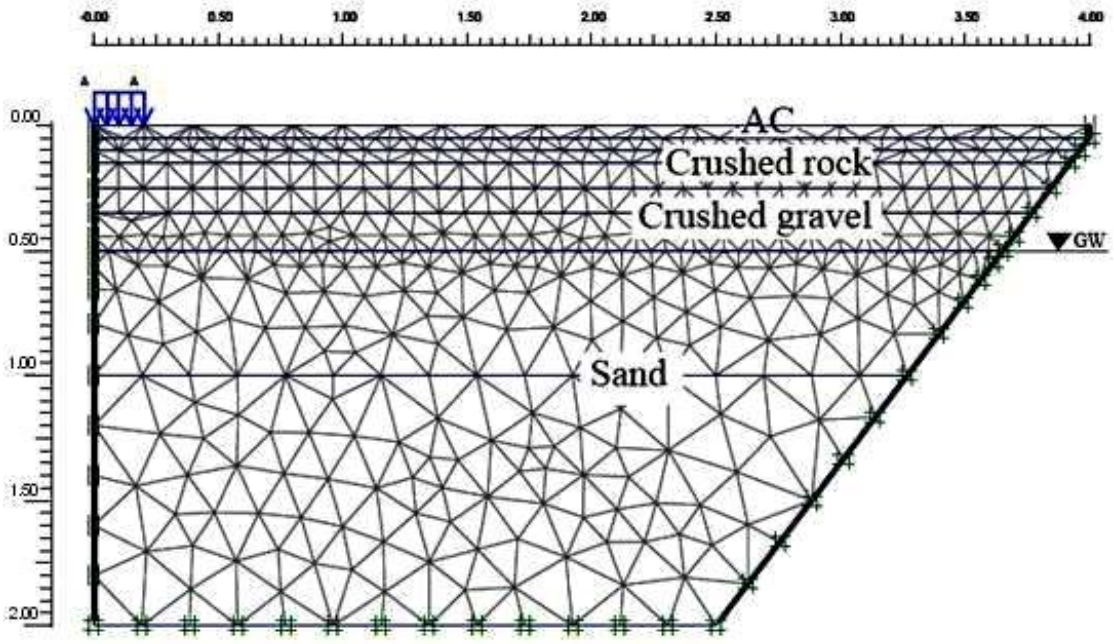

Figure 2: Element mesh and boundary conditions of the unreinforced model.

In these models, the attention was paid to the stress distributions and to the resilient deformations. All analyses carried out were static. The dynamic analysis was not carried out because the dynamic module of the Plaxis program is not suitable for modeling of traffic loading (Korkiala et al., 2003).

The reinforced structure was modeled with the same properties of unreinforced model but geogrid reinforcement placed in three different locations to study the effect of geogrid location in tension stress absorption. To start with, the geogrid was placed under the asphalt layer (Y = 0.05 m), under the base layer (Y = 0.25 m) and finally located under sub-base layer (Y = 0.5 m). The element mesh and boundary conditions of the reinforced structure are shown in Figure 3.

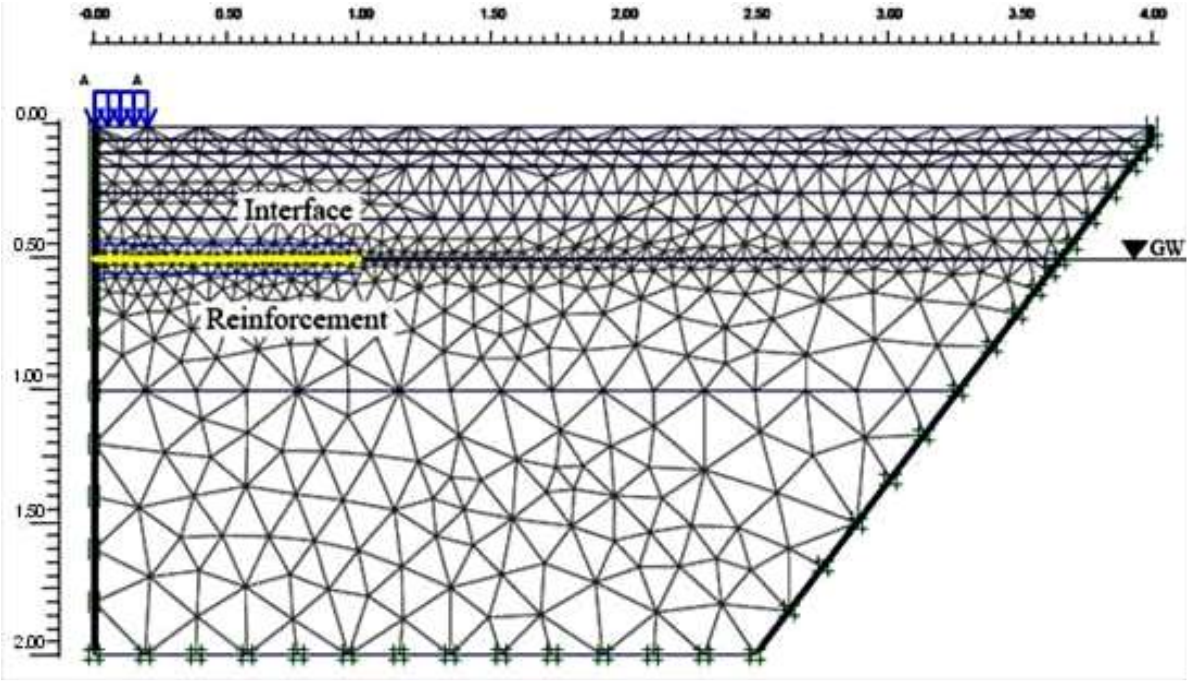

Figure 3: Element mesh and boundary conditions of reinforced model (Y = 0.5 m).

REINFORCEMENT PROPERTIES

The various properties of geogrid are shown in Table 2.

Table 2: Properties of geogrid.

Parameters	
Geogrid type	BX-1100
Polymer	Polypropylene
Aperture shape	Rectangle
Aperture size (MD/XD)(mm)	25/33
Rib thickness (mm)	0.75
Junction thickness(mm)	2.8
Tensile strength at 5% strain (kN/m)	
MD	8.46

XD	13.42
Initial modulus (kN/m^2)	
MD	226.4
XD	360.1
Long term allowable strength in crushed aggregate	
MD	N/A
MD = machine direction	
XD = cross machine direction	

RESULTS AND DISCUSSION

The results of the modeling are presented in Figures 4 to 11. Figure 4 shows the variation of the shear stress in interface with distance from the load for geogrids placed at various locations. The maximum shear stress in the interface is 21.5 kpa for geogrid placed at a distance of 0.5 m from the bottom of the model, 57.3 kPa at 0.25 m and 157.4 kPa at 0.05 m. It was clear that the geogrid placed at the bottom of asphalt layer (Y = 0.5 m) has increased surprisingly the shear stress in the interface (Barksdale et al., 1989; Ling and Liu, 2003). These stresses will be transferred to geogrid as tension stress.

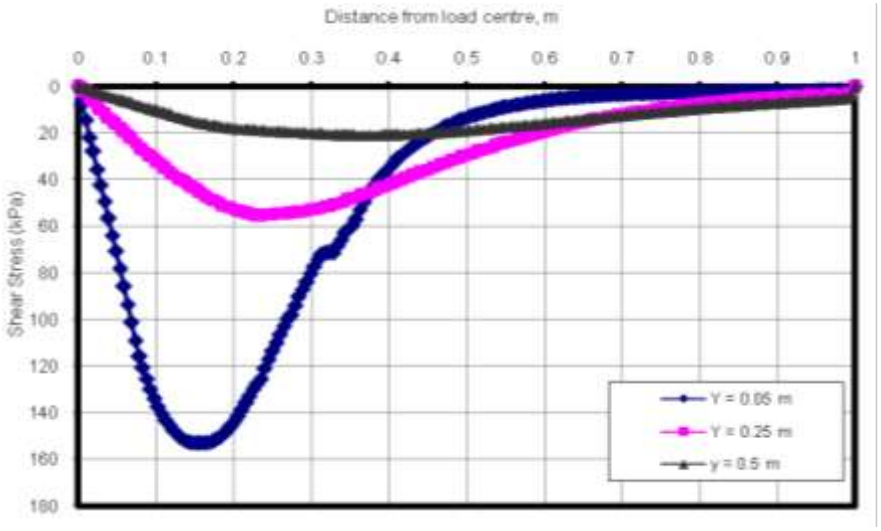

Figure 4: Effect of different locations of geogrid on shear stress absorption of shear interface).

The variation of effective normal stress in shear interface of soil-geogrid from the load is shown in Figure 5. The effective normal stress for the geogrid place at 0.5 m from the base of the model is 84 kPa, 190 kPa at 0.25 m and 460 kPa at 0.05 m. High normal stresses on the center of loading can produce high shear stresses at shear interface as shown in Figure 4.

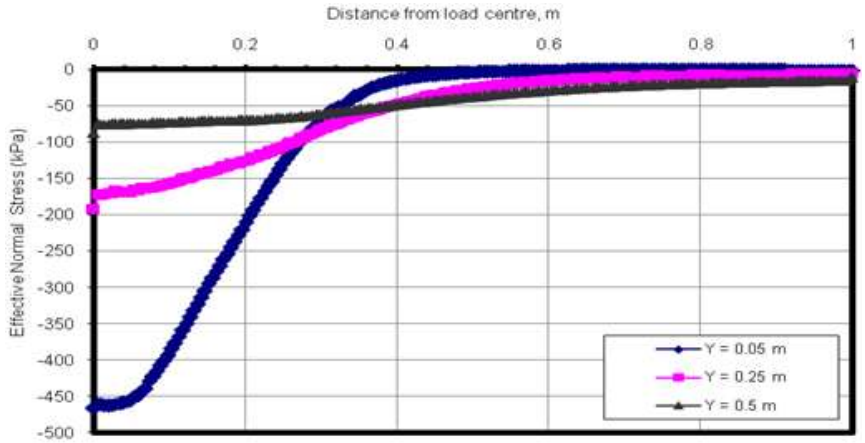

Figure 5: Effect of location of geogrid on normal stress at the interface.

The vertical deflection of geogrids with distance from the load is shown in Figure 6. The deflection observed under the centre of the load for unreinforced model is 1.16 mm and this reduces to 0.0019 mm with the use of geogrid just under the asphalt layer.. This shows the effectiveness of geogrid in controlling the deflection when used just below the asphalt layer.

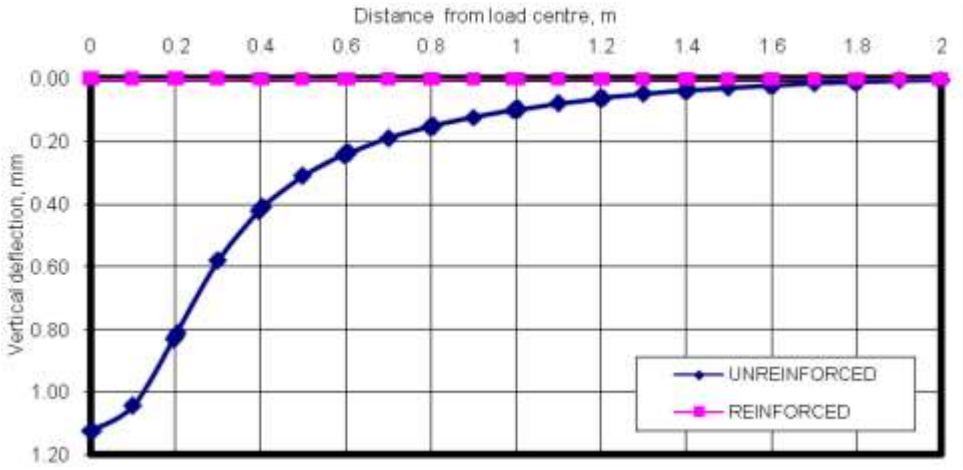

Figure 6: Vertical deflections for unreinforced and reinforced model.

In Figure 7, the results of vertical deflection of the geogrids for three locations of the reinforcement are presented as a comparison to find out the location which gives the least vertical deflection. The results were quiet surprising because it showed very identical deflections.

The deflections were about 0.0019 mm under the center of the load and decreasing sharply to about 0.0001 mm at 0.3 m from the center of the load. However, there were differences in tension absorption. In fact these analyses are valid only for the cases where permanent strains during one loading cycle are an insignificant part of resilient strains.

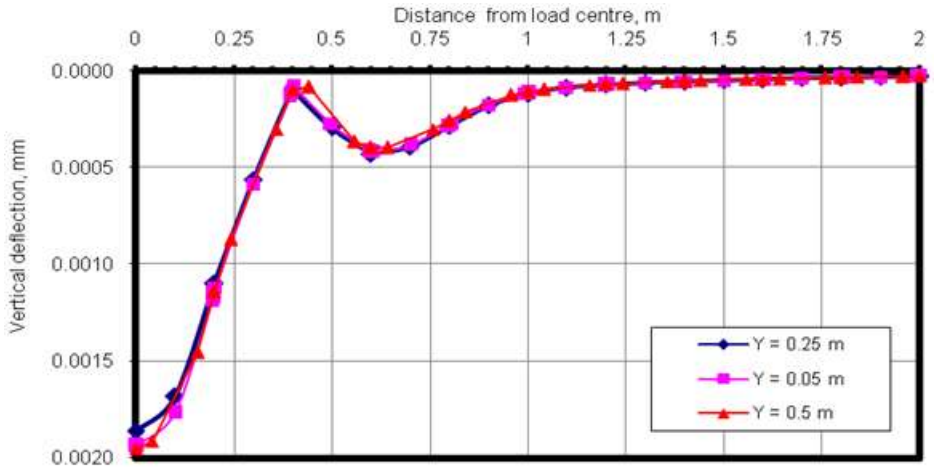

Figure 7: Vertical deflections in model with geogrid at three different locations.

Figures 8 to 11 show the locations of plastic and tension-cut-off points developed in the reinforced and unreinforced models for the same conditions. It was observed that similar results were also seen in Figures 5 and 6. The tension cut-off points in reinforced structure were concentrated close to the reinforcement layers. The magnitude of concentration was observed to increase when using the reinforcements close to the load applied. This indicates that the load applied was taken up by the geogrids. The effectiveness of geogrids is more pronounced when it is placed at the bottom of the asphalt concrete.

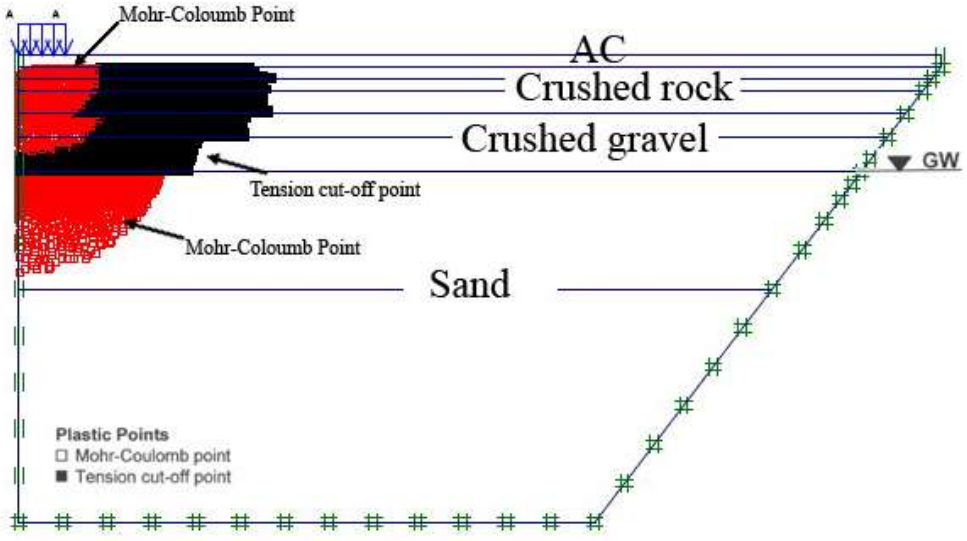

Figure 8: Plastic and tension cutoff points (unreinforced).

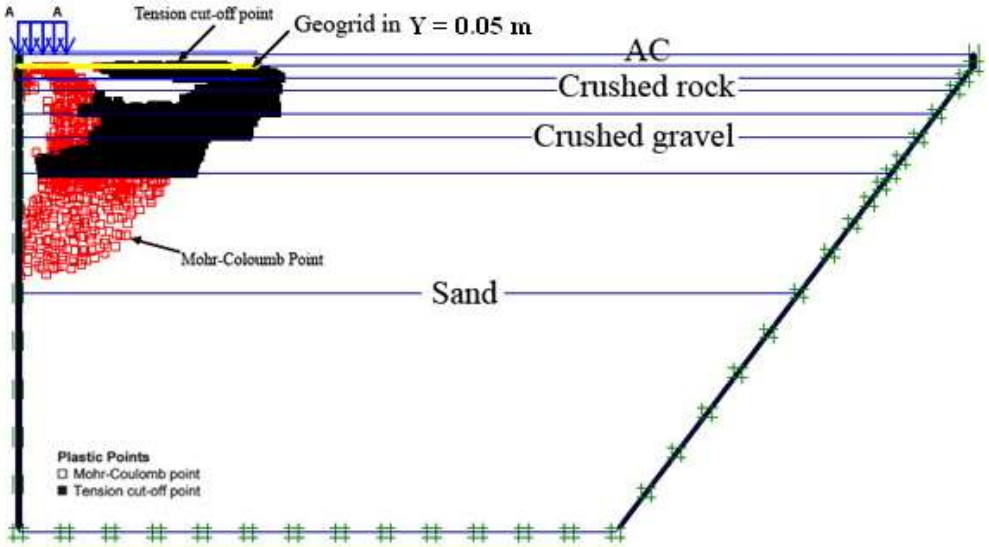

Figure 9: Plastic and tension cut off points (reinforcement at Y = 0.05 m).

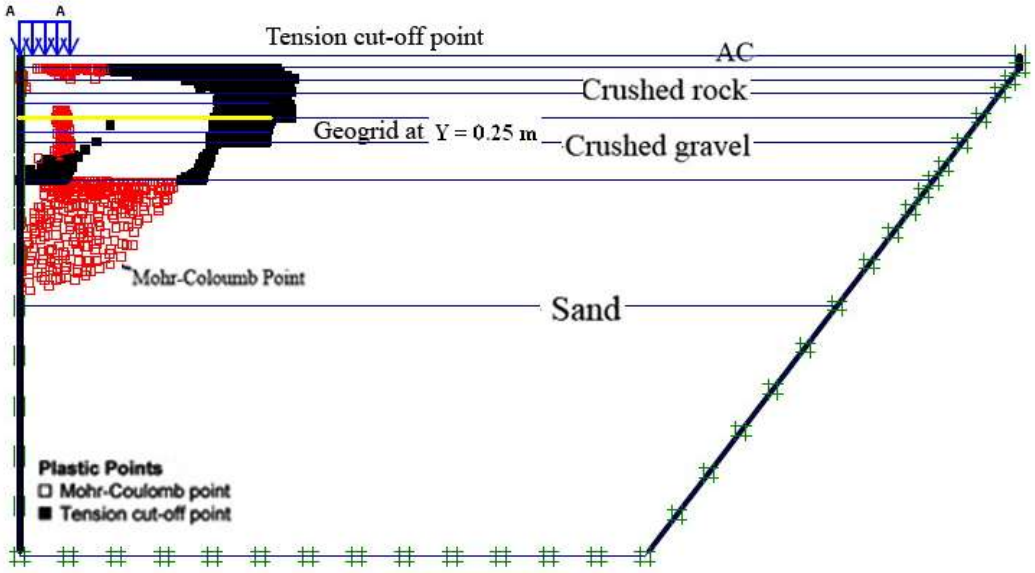

Figure 10: Plastic and tension cut off points (reinforcement at Y = 0.25 m).

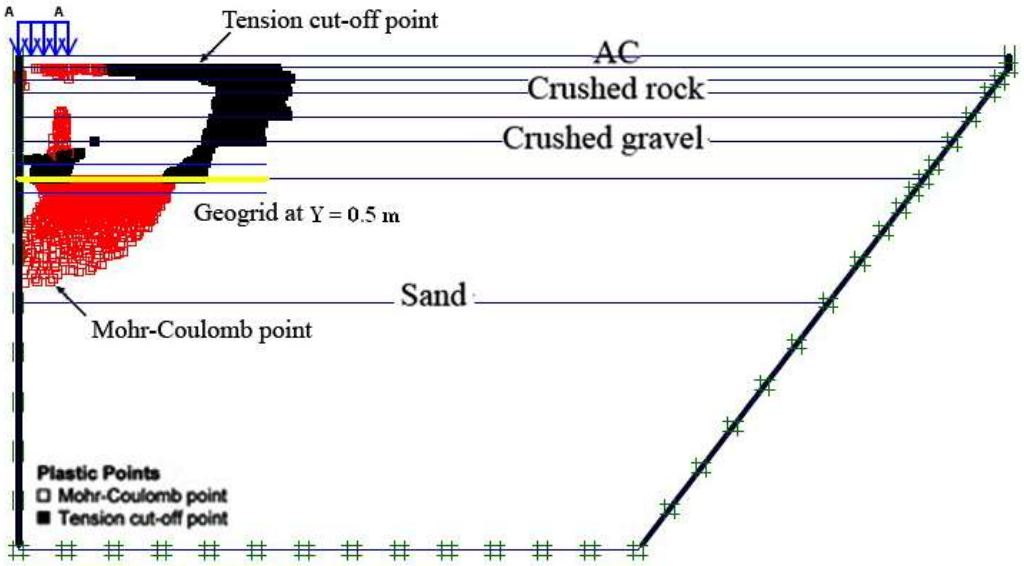

Figure 11: Plastic and tension cut off points (reinforcement at Y = 0. 5 m).

CONCLUSIONS

A finite element representation of geogrid is presented for the analysis of soil-geogrid interaction system. The technique is used in association with a two-dimensional axisymmetric finite element type of analysis to study the behavior of geogrids embedded in paved roads. The results showed the restraining effects of geogrid in the asphalt pavement system. When the load is applied to the surface of the pavement, a zone of tension is developed at the lower section of the asphalt concrete layer. To improve the rigidity of the asphalt concrete layer, which may be considered as a beam, the geogrid is included as tensile reinforcement. The tensile stress acting in the asphalt concrete is thus transferred to the geogrid as tensile force. When the geosynthetic reinforcement is placed at the bottom of the asphalt concrete layer, it leads to the highest reduction in the vertical deflection. The overall performance of the asphalt pavement is improved if an effective bonding is maintained between the asphalt concrete and geogrid. Also, the settlement over the loading area of reinforced pavement reduced when compared with unreinforced pavement.

REFERENCES

1. ASTM, American Society for Testing Materials (2000) "Standard Specification for Materials for Soil – Aggregates Sub base, Base, and Surface Courses," *Designation: D 11241–94*.
2. Barksdale, R. D., S.F. Brown, and F. Chan (1989) "Aggregate base reinforcement of surfaced pavement," *Geotextiles and Geomembranes*, Vol. 8, pp 165–189.
3. Broms, B. B. (1977) "Triaxial tests with fabric-reinforced soil," Proc. Int. Conf. on the Use of Fabric in Geotechnics, Ecole National des Ponts et Chaussees, Paris, Vol. 3, pp 129–134.
4. Carotti, A. and P. Rimoldi (1998) "A nonlinear model for the seismic response analysis of geosynthetic-reinforced soil structures," Geosynthetics International J., Vol. 5, Nos. 1-2, pp 167-201.

5. Chan, F., R.D. Barkesdale, and S.F. Brown (1989) "Aggregate base reinforcement of surfaced pavements," Int. J. Geotextiles Geomembrane, Vol. 8, pp 165–189.
6. Dondi, G. (1994) "Three-dimensional finite element analysis of a reinforced paved road," Proc., Fifth International Conference on Geotextiles, Geomembranes, and Related Topics, Vol. 1, pp 95-100.
7. Giroud, J. P., C. Ah-Line, and R. Bonaparte (1985) "Design of unpaved roads and trafficked areas with geogrids," Proc. Symp. Polymer Grid Reinforcement, Science and Engineering Research Council and Netlon Ltd., London, pp 116–127.
8. Haliburton, T. A. and J.V. Baron (1983) "Optimun-depth method for design of fabric-reinforced unsurfaced roads," Transportation Research Record 916, pp 26-32.
9. Hansen, R. W., C. Bertrand, K.M. Marshek, and W.R. Hudson (1989) "Truck tire pavement contact pressure distribution characteristics for super single 18-22.5 and smooth 11R24.5 tires," Rep. 1190-1, Center for Transportation Research, Univ. of Texas at Austin, Austin, Tex.
10. Korkiala-Tanttu, L., R. Laaksonen, and J. Törnqvist (2003) "Effect of spring and overload to the rutting of a low-volume road," HVS-Nordic – research, Finnra Reports 22.
11. Kuo, M. C., K.T. Hall, and M. Darter (1995) "Three-dimensional finite element model for analysis of concrete pavement support," Transportation Research Record 1505, Transportation Research Board, National Research Council, Washington, D.C., pp 119–127.
12. Ling, H. I. and H. Liu (2003) "Finite element studies of asphalt concrete pavement reinforced with geogrid," J. Eng. Mech., Vol. 129, No. 7, pp 801–811.
13. Milligan, G. W. E. and J.P. Love (1984) "Model testing of geogrids under and aggregate layer on soft ground," Proc., Polymer Grid Reinforcement Conference, Thomas Telford, London, pp 128-138.
14. Miura, N., A. Sakai, and Y. Taesiri (1990) "Polymer grid reinforced pavement on soft caly grounds," Geotextile and Geomembranes, Vol. 9, pp 99-123.
15. Perkins, S.W. (1999) "Mechanical response of geosynthetic-reinforced flexible pavements," Geosynthetics International, Vol. 6, No. 5, pp 347-382.
16. Perkins, S. W. (2001) "Numerical modeling of geosynthetic reinforced flexible pavements: Final report," Rep. No. FHWA/MT-01/003/ 99160-2, Montana Department of Transportation, Helena, Mont.
17. Saad, B., H. Mitri, and H. Poorooshasb (2006) "3D FE analysis of flexible pavement with geosynthetic reinforcement," Journal of Transportation Engineering, American Society of Civil Engineers, Vol. 132, No. 5, pp 402-415.
18. Steen, E. R. (2004) "Stress relieving function of paving fabrics when used in new road construction," Proc., 5th International RILEM Conference, Edited by C. Petit, I.L. Al-Qadi, and A. Millien, Limoges, France, pp 105-112.
19. Wathugala, G. W., B. Huang, and S. Pal (1996) "Numerical simulation of geogrid reinforced flexible pavements," Transportation Research Record 1534, Transportation Research Board, National Research Council, Washington, D.C., pp 58–65.
20. Yoder, E. J. and M.W. Witczak (1975) "Principles of pavement design," 2nd Ed., Wiley, New York.